Numerical sampling of extreme drag fluctuations on obstacles in turbulent flows

T. Lestang[a], F. Bouchet[b], E. Lévêque[c]

a. Univ Lyon, Ens de Lyon, Univ Claude Bernard, CNRS, Laboratoire de Physique, F-69342 Lyon, France, thibault.lestang@ens-lyon.fr
b. Univ Lyon, Ens de Lyon, Univ Claude Bernard, CNRS, Laboratoire de Physique, F-69342 Lyon, France, freddy.bouchet@ens-lyon.fr
c. Univ Lyon, Ecole Centrale de Lyon, Univ Claude Bernard, CNRS, Laboratoire de Mécanique des Fluides et d'Acoustique, F-69134 Ecully cedex, France, emmanuel.leveque@ec-lyon.fr

Résumé :

Nous proposons une approche originale pour l'étude numérique des fluctuations extrêmes de trainée sur un obstacle immergé dans un écoulement turbulent. L'approche se base sur un algorithme d'événements rares couplé à la simulation numérique directe de l'écoulement. L'algorithme suit l'évolution d'une population de simulations indépendantes et les duplique/supprime périodiquement de manière à favoriser les fluctuations extrêmes de la trainée moyennée sur un temps donné. Nous appliquons cet algorithme à un écoulement simple et calculons la statistique et la dynamique correspondant à des fluctuations rares avec un coût numérique grandement réduit comparé à celui requis par une longue simulation numérique directe.

Abstract :

We propose a novel way to conduct the numerical study of extreme drag fluctuations over an obstacle immersed in a turbulent flow. It is based on a rare event sampling algorithm and direct numerical simulation of the flow. The algorithm tracks the evolution of an ensemble of independent simulations and periodically duplicate/discard some of them to favour trajectories related to extreme fluctuations of the average drag over a given duration. We apply this algorithm to a simple flow and compute statistics and dynamics of rare fluctuations with a greatly reduced computational cost compared to direct sampling from one long direct numerical simulation.

Keywords : Turbulence, Drag fluctuations, Rare events, Importance Sampling, Large deviations

1 Introduction

A striking property of turbulent flows is the sporadic occurrence of extremely intense fluctuations in pressure or velocity fields, and forces on objects. Such fluctuations can induce extreme mechanical

efforts on immersed obstacles such as drag, lift or torque. Statistics and dynamics of fluctuating mechanical efforts are of relevant interest in mechanical engineering, where the modelling, understanding and predictability of aerodynamics around bluff bodies are of crucial matter. Examples include the study of drag and lift fluctuations affecting road vehicles [14, 2], estimation of wind loads on structures such as tall buildings and bridges [11] and the effect of the intermittent nature of the atmospheric boundary layer on wind energy production [10, 18, 8].

These issues are traditionally investigated through experiments that can be time-consuming, costly and hard to carry out with precision, especially if a small scale model cannot be built. An alternative is computational modelling based on a suitable mathematical model. Unfortunately, long range spatio-temporal correlations responsible for the rare occurrence of large fluctuations are very difficult to capture numerically. For the sake of simplicity, statistics of such events are often considered to be Gaussian, leading to a major underestimation of the impact of repetitive occurrence of rare fluctuations. The best practice would be to simulate the flow from first principles (the Navier-Stokes equations). This approach is referred to as Direct Numerical Simulation (DNS). However, the tremendous computational cost associated with the DNS of turbulence makes it unpractical for the study of rare events that would require to simulate the flow over a very long time.

In this paper we propose a novel way to perform computational studies of rare fluctuations in turbulent flows, bypassing the requirement of very long DNS. The problem of computing the statistics and dynamics associated to rare events has been extensively studied in statistical mechanics. A key theoretical tool is *Large Deviation Theory* which deals with rates at which probabilities of rare fluctuations decay as a function of a given parameter [17]. Recently, significant efforts have been made to design numerical methods to compute rare events in different fields of research. They have been applied for instance to investigate changes of configurations in magnetic systems in situations of first order transitions [5, 7], chemical reactions [3], conformal changes of polymer and bio-molecules [13, 9, 1, 19]. The objective of our work is to assess the practicality of such algorithms to compute rare events in realistic complex systems involving a large number of degrees of freedom, such as turbulent flows.

We compute extreme fluctuations for the *time averaged* drag

$$F_T(t) = \frac{1}{T} \int_t^{t+T} f(t')\mathrm{d}t'$$

where f is the instantaneous drag force acting on an obstacle immersed in a flow. In this paper, we mostly focus on the drag averaged over a duration T much bigger than the correlation time of typical fluctuations, for reasons that will be made clear in section 2. To establish a proof of concept, we test the approach on a simple flow. In section 2, we briefly present the aforementioned algorithm and describe its relation with *Large Deviation Theory*. Next, section 3 introduces the computational setup on which our numerical experiments were carried out and gives the essence of the computational method we used to simulate the flow, namely the *Lattice Boltzmann Method*. Eventually, section 4 illustrates the validity of the method and its efficiency, as well as the results for the generation of extreme drag fluctuations.

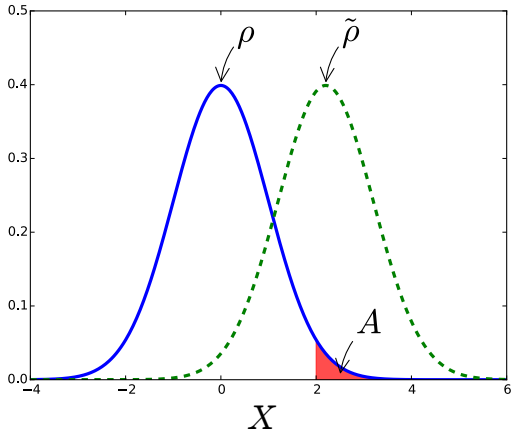

FIGURE 1 – Let X be a realisation of a process following the probability density ρ. We address the problem of computing the probability $\mathcal{P}(X \in A)$ that X falls into the region A. Direct sampling of the distribution ρ would require a huge number of realisations to yield a reliable estimate of $\mathcal{P}(X \in A)$ since the latter is very small. *Importance Sampling* is a technique that consists in sampling another distribution $\tilde{\rho}(X) = \mathcal{L}(X)\rho(X)$ where $\mathcal{L}$ is chosen so that typical realisations of the process following $\tilde{\rho}$ fall into A.

2 Importance Sampling

We address the problem of studying the probability density function of the average drag

$$\mathcal{P}\left(\frac{1}{T}\int_t^{t+T} f(t')dt' = a\right) \tag{1}$$

and the dynamics leading to the related events. Direct sampling of this probability density function can be achieved by performing an ensemble of simulations of the flow. This yields an ensemble of trajectories distributed according to the trajectory probability measure $P^{(0)}\left(\{X(t)\}_{0<t<T} = \{x(t)\}_{0<t<T}\right)$, where a trajectory refers to a dynamical solution of the numerical model with $X(t)$ a vector that contains information about all the degrees of freedom of the model at time t. However, direct sampling proves very inefficient since it would require simulation of the flow over very long times, entailing tremendous computational effort.

2.1 Importance sampling at the level of trajectories

In order to sample the tails of the distribution (1) efficiently, we turn instead to *importance sampling*. Importance sampling is a general technique for drawing realisations from a distribution, focusing on a specific (*important*) region. Figure 1 illustrates the idea of importance sampling applied to the sampling of the tails of a specified distribution of probability. Instead of generating trajectories according to $P^{(0)}\left(\{X(t)\}_{0<t<T} = \{x(t)\}_{0<t<T}\right)$, we generate an ensemble of trajectories according to a modified probability $P_k\left(\{X(t)\}_{0<t<T} = \{x(t)\}_{0<t<T}\right)$

$$P_k\left(\{X(t)\}_{0<t<T} = \{x(t)\}_{0<t<T}\right) = \frac{\exp\left(k\int_0^T f_j[\mathbf{x}(t)]dt\right)}{\left\langle \exp\left(k\int_0^T f_j[\mathbf{x}(t)]dt\right)\right\rangle} P^{(0)}\left(\{X(t)\}_{0<t<T} = \{x(t)\}_{0<t<T}\right) \tag{2}$$

where $\langle . \rangle$ indicates averaging over the density $P^{(0)}\left(\{X(t)\}_{0<t<T} = \{x(t)\}_{0<t<T}\right)$. This way, trajectories are assigned a weight that is proportional to the corresponding value of $\int_0^T f[\mathbf{x}(t)]dt$. Generating

trajectories sampled according to $P_k\left(\{X(t)\}_{0<t<T} = \{x(t)\}_{0<t<T}\right)$ thus favours the occurrence of trajectories with extreme values of $\int_0^T f[\mathbf{x}(t)]dt$.

This is done by simulating an ensemble of N_c copies of the flow, each of them starting from independent initial conditions. Each copy (labelled by an index j) is then simulated from $t = 0$ to an arbitrary time $t = \tau$. Next, each copy is replicated or discarded so that, *in average*, it gives birth to n_j clones with

$$n_j = \frac{\exp\left(k\int_0^\tau f_j[\mathbf{x}(t)]dt\right)}{\frac{1}{N}\sum_{l=1}^N \exp\left(k\int_0^\tau f_l[\mathbf{x}(t)]dt\right)} \tag{3}$$

This yields an ensemble of trajectories distributed according to the distribution

$$P^{(1)}\left(\{X(t)\}_{0<t<\tau} = \{x(t)\}_{0<t<\tau}\right) = \frac{\exp\left(k\int_0^\tau f_j[\mathbf{x}(t)]dt\right)}{\frac{1}{N}\sum_{j=1}^N \exp\left(k\int_0^\tau f_j[\mathbf{x}(t)]dt\right)} P^{(0)}\left(\{X(t)\}_{0<t<\tau} = \{x(t)\}_{0<t<\tau}\right)$$

Besides, when N_c is large we have, up to fluctuations of order $\sqrt{N_c}$

$$\frac{1}{N}\sum_{j=1}^N \exp\left(k\int_0^\tau f_j[\mathbf{x}(t)]dt\right) \approx \left\langle \exp\left(k\int_0^\tau f_j[\mathbf{x}(t)]dt\right)\right\rangle \tag{4}$$

The clones then evolve from τ to 2τ and the cloning step is repeated, yielding an ensemble of trajectories distributed according to $P^{(2)}\left(\{X(t)\}_{0<t<2\tau} = \{x(t)\}_{0<t<2\tau}\right)$. Eventually , after $N = \frac{T}{\tau}$ iterations of the evolution/selection process, one obtains a ensemble of trajectories distributed according to the tilted probability (2). See [12] for a more detailed discussion of the algorithm.

2.2 Drag averaged over a long time and large deviation results

We now elaborate on the special case where the drag is averaged over a duration much longer than the typical timescale of the turbulent fluctuations. In this case, one can show that

$$\frac{1}{T}\ln \mathcal{P}\left(\frac{1}{T}\int_t^{t+T} f(t')dt' = a\right) \underset{T\to\infty}{\longrightarrow} I(a) \tag{5}$$

We say that the distribution satisfies a *large deviation principle*. The limit $T \to \infty$ is to be understood as $T >> \tau_c$, where τ_c is the timescale of the the turbulent fluctuations. The function $I(a)$ is called the *rate function* and encodes the statistics of the averaged drag, from common fluctuations to the far tails of the distribution. The large deviation principle can be seen as an extension of the Central Limit Theorem, as it describes the Gaussian fluctuations of order $1/\sqrt{T}$, but also the tails of the distribution and the corresponding rate of decrease. At this point it is useful to define the *Scaled Cumulant Generating Function* (SCGF)

$$\lambda(k) = \lim_{T\to\infty} \lambda(k,T) \text{ with } \lambda(k,T) = \frac{1}{T}\ln\left\langle \exp\left(k\int_0^{T_a} f_j[\mathbf{x}(t)]dt\right)\right\rangle$$

The SCGF is directly linked to the rate function : $I(a) = k_a a - \lambda(k_a)$ with $\lambda'(k_a) = 0$.

The rate function can be computed by the algorithm. Its main output is the value of the SCGF for the value of k prescribed to weight the trajectories (see equations (2) and (3)). This can be seen by taking

the long time limit in (2) :

$$P_k\left(\{X(t)\}_{0<t<T} = \{x(t)\}_{0<t<T}\right) = \frac{\exp\left(k\int_0^T f_j[\mathbf{x}(t)]dt\right)}{e^{T\lambda(k)}} P^{(0)}\left(\{X(t)\}_{0<t<T} = \{x(t)\}_{0<t<T}\right)$$

Eventually, using (4), $\lambda(k)$ can be connected to the averaged drag over each evolution process

$$e^{T\lambda(k)} \approx \frac{1}{N}\sum_{j=1}^{N} \exp\left(k\int_0^{\tau} f_j[\mathbf{x}(t)]dt\right) \times \frac{1}{N}\sum_{j=1}^{N} \exp\left(k\int_{\tau}^{2\tau} f_j[\mathbf{x}(t)]dt\right) \times ... \tag{6}$$

In the next, we focus on the long-time averaged drag on an obstacle in flow. The correct computation of the SCGF will serve as a validation for the algorithm.

3 Numerical setup

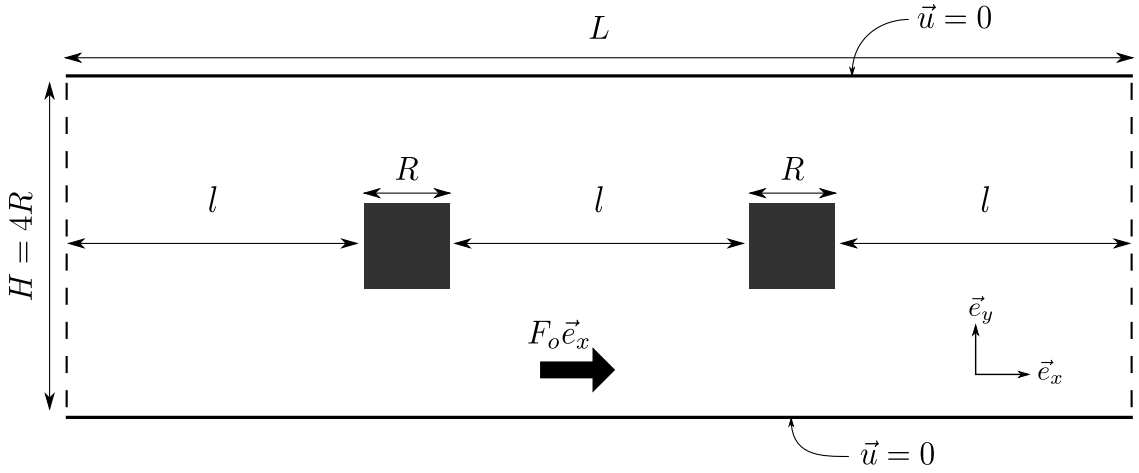

FIGURE 2 – Sketch of the (two-dimensional) computational domain. Periodic boundary conditions at the inlet/outlet are implemented and therefore the flow in the computational domain corresponds to the flow in an infinite pipe, containing an infinite chain of obstacles. The flow is driven by a uniform body force aligned with the axis of the pipe. We use $N_y = 129$ grid points in the cross-flow direction and $N_x = 385$ grid points in the flow direction. The Reynolds number is $Re = \frac{U_0 R}{\nu} = 700$ with U_0 the mean flow velocity in stationary regime.

We focus on the two-dimensional flow around two equally spaced squares cylinders in a pipe, as shown in figure 3. The flow is simulated using the *Lattice Boltzmann Method*.

The Lattice Boltzmann Method (hereafter mentioned as LB method) offers a computationally efficient particle-based alternative to conventional *continuum*-based approaches to simulate fluid dynamics [16]. The fluid is considered at a kinetic level intermediate between the microscopic and the macroscopic. More precisely, the fluid is viewed as populations of particles that collide, redistribute and propagate along the different links of a discrete lattice. The complexity of the flow emerges from the repeated application of simple rules of collision and streaming of these populations at each lattice node. The flow variables such as velocity and pressure are obtained by averaging locally over the populations of

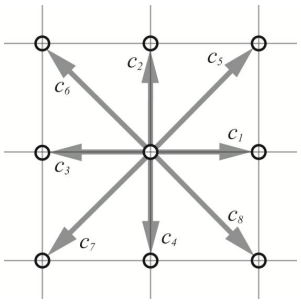

FIGURE 3 – Discrete directions linking the lattice nodes, along which particles can move.

particles moving in the different directions (Fig. 3). This obviously refers to a kinetic description of fluid dynamics and rigorous connections can be established with the Boltzmann equation (under the so-called BGK approximation) [4].

Formally, the LB scheme reads (under the BGK approximation for the collision kernel) as

$$f_i(\mathbf{x}+\mathbf{c}_i\Delta t, t+\Delta t) \quad = \quad f_i(\mathbf{x},t) - \frac{1}{\tau}\left[f_i(\mathbf{x},t) - f_i^{eq}(\mathbf{x},t)\right] + \Delta t \mathcal{F}_i \qquad \text{for } i=0,\ ...8 \tag{7}$$

$$\tag{8}$$

where $f_i(\mathbf{x},t)$ represent the amount of mass (per unit volume) carried by the particles moving (with speed $\mathbf{c}_i$) in the i^{ts}-direction at position $\mathbf{x}$ and time t. The term $\mathcal{F}_i$ [6] allows us to account for the presence of a body force, namely $\mathbf{Q}$, that is

$$\mathcal{F}_i = \left(1-\frac{1}{2\tau}\right) w_i \left[\frac{\mathbf{c}_i - \mathbf{u}}{c_s^2} + \frac{\mathbf{c}_i\cdot\mathbf{u}}{c_s^2}\mathbf{c}_i\right]\cdot\mathbf{Q}. \tag{9}$$

The macroscopic quantities are recovered locally by summing the contributions

$$\rho \quad = \quad \sum_i f_i \tag{10}$$

$$\rho\mathbf{u} \quad = \quad \sum_i f_i\mathbf{c}_i + \frac{1}{2}\mathbf{Q}\Delta t \tag{11}$$

$$\tag{12}$$

The pressure is intrinsically given by $P = c_s^2\rho$ in a weak-compressibility approximation, where c_s may be interpreted as the speed of sound. The relaxation parameter τ is related to the kinematic viscosity of the fluid : $\tau = 1/2 + \nu/\Delta t c_s^2$.

The instantaneous drag is computed at each time-step by integrating the strain rate tensor on the surface of the obstacle and projecting along the direction of the flow. Figure 4 shows snapshots of the velocity and vorticity fields, respectively.

4 Computation of statistics for rare drag fluctuations

We finally present and discuss the application of the importance sampling method described in section 2 to the study of extreme drag fluctuations. We use the numerical setup introduced in the previous

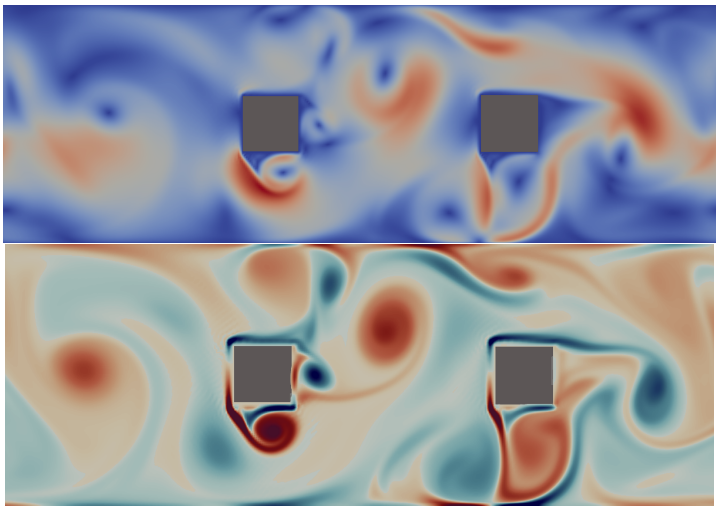

FIGURE 4 – Typical realisation of velocity and vorticity fields. **Top** : Velocity field. **Bottom** : Vorticity field

section and focus on the averaged drag on one of the square obstacles.

Applying the importance sampling algorithm presented in section 2 with deterministic dynamics, one must add some randomness in the evolution of the clones for them to separate during the evolution process. In this work, we simply perturb the initial state of new clones and let the chaoticity of the flow separate the trajectories.

4.1 Validation of the method and quantification of its efficiency

In order to validate the proposed approach we first compute an estimate of the SCGF from a long direct numerical simulation of the flow, referred to a the *control run*. This estimate will serve as a benchmark. Then, for a lower computational cost, we compare the result from the importance sampling on the one hand, and direct numerical simulation on the other hand. We express computational costs in terms of *turn-over time*. The turn-over time is the typical timescale of advection by the mean-flow.

We perform a control run with a cost $C_{long} = 2.3 \times 10^6$ turn-over times and compute a direct estimate of the SCGF. The latter is obtained by dividing the time series in blocks of length ΔT, with ΔT much longer than the typical correlation time of the instantaneous drag fluctuations, so that the large deviation regime (5) is reached. We can then compute an estimator of the SCGF.

$$\hat{\lambda}(k) = \frac{1}{T} \ln \frac{1}{M} \sum_{m=1}^{M} \exp\left(k \int_{m\Delta T}^{(m+1)\Delta T} f(t) \right) \ , \ M = \frac{T}{\Delta T}$$

Due to the finite size of the time series, the estimator $\hat{\lambda}$ can only be trusted between two threshold values k_{min} and k_{max}, past which convergence of the estimator cannot be established. We redirect the interested reader to [15]. In the next, we will only focus on positive values of k, *i.e.* positive fluctuations of the average drag.

We then perform simulations using the importance sampling algorithm with a cost $C_{short} << C_{long}$. The cost of a run of the importance sampling algorithm corresponds to $N_c \times T_a$, that is the number of clones times the total time over which each clone is simulated. Lastly, a direct estimation with the same cost C_{short} is carried out. The results obtained from the validation protocol are shown in figure 5. Figure 5 illustrates that a good estimation of the SCGF is achieved at a much lower computational cost C_{short}, whereas direct numerical simulation for cost C_{short} is restricted to lower values of k, that is events closer to typical fluctuations.

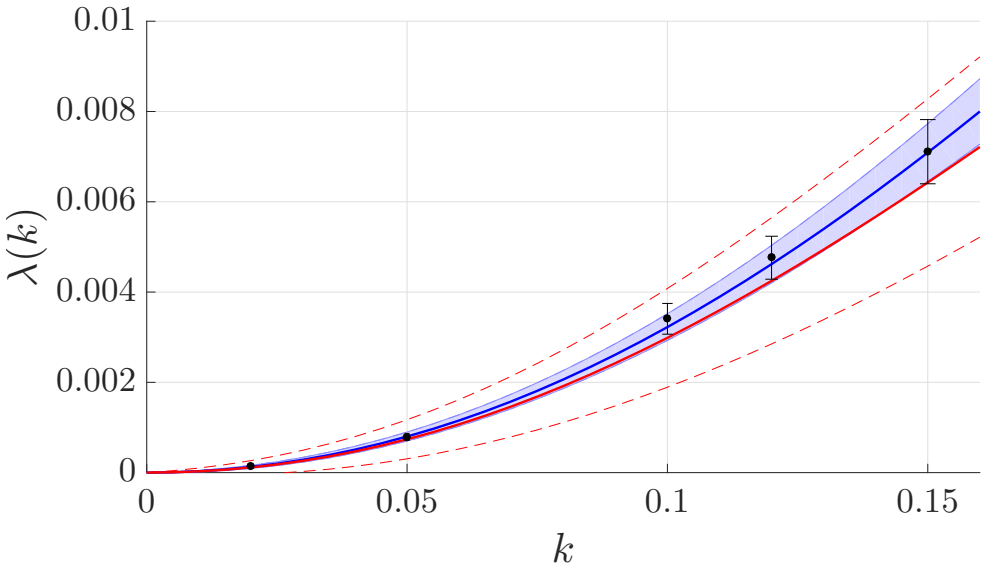

FIGURE 5 – Scaled Cumulant Generating Function obtained from three different methods. The thick blue line represents the estimate computed from a long direct numerical simulation with a computational cost $C_{long} = 2.3 \times 10^6$ turn-over times. Black dots correspond to the output of the importance sampling algorithm with 128 replica, simulated over 400 turn-over times leading to a total cost of $C_{short} = 5.12 \times 10^4$ turn-over times. The cloning period is $\tau = 0.5$ turn-over times. Finally, the thick red line represents the estimate obtained from a direct numerical simulation with cost C_{short}. Dashed red lines and thin blue lines mark out the confidence region for both estimations. The blue estimate can only be trusted up to $k \approx 0.16$, after which the convergence of the estimator cannot be easily established and errors cannot be quantified. This figure illustrates that the algorithm is able to compute the value of the SCGF up to such values of k at a much lower computational cost.

The upper bound of the control run is reached for $k = 0.15$. For trajectories of length $T_a = 400$ turn-over times, this corresponds to fluctuations of $\frac{1}{T_a}\int_t^{t+T_a} f(t')dt'$ being more than 2 standard deviations σ away from the average value.

4.2 Discussion of the algorithm efficiency

To sum up, our experiment shows that for fluctuations being more than 2σ away than the average value, the SCGF is computed for 3% of the computational effort required by a direct estimation. We stress here that the cost of the importance sampling algorithm does not depend much on k, that is the on the rarity of the typically sampled events. In comparison, the cost of a direct estimation grows like the inverse of the probability of the corresponding rare events, and thus the algorithm efficiency is expected to increase like the inverse of the probability of the events. In practice however, the improvement is slightly slower than the inverse of the probability of the events. The rarer the events (the higher $|k|$), the more stringent

is the selection imposed by the algorithm. As a consequence, one has to increase the number of clones or/and reduce the cloning time. Reducing the cloning time does not *a priori* impact the computational cost of the method. However, this is true only if one can neglect the cost of the cloning step compared to the evolution step and low cloning times can significantly increase the computational effort required to run the algorithm.

4.3 Reconstruction of dynamics related to extreme fluctuations

As mentioned in section 2, the selection imposed by the algorithm results in an ensemble of trajectories distributed according to a modified probability (2). From the final state of the ensemble of copies, the trajectories are reconstructed by tracing back in time the evolution of the replica, following the evolution of the ancestors of every clone. It is then possible to compute the average drag over these trajectories and verify that the distribution of these values is shifted towards extreme fluctuations. Figure 6 shows the ensemble of values for the average drag obtained with the algorithm after reconstructing trajectories.

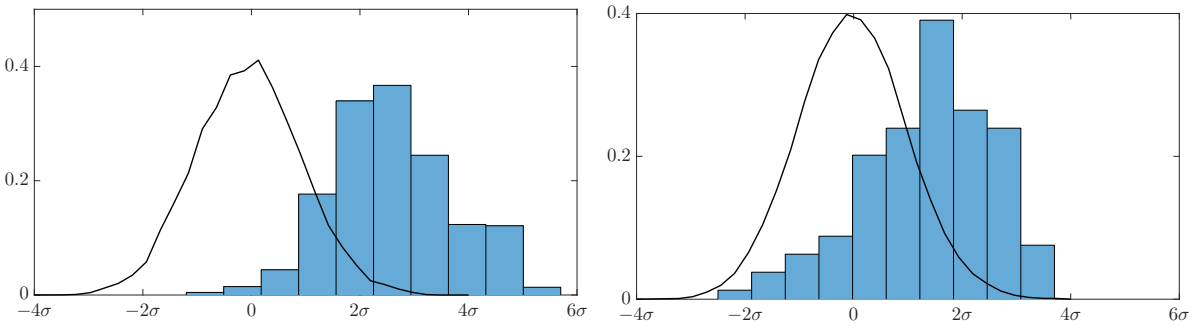

FIGURE 6 – In blue, the values of the average drag over the trajectories generated by the importance sampling algorithm. The thick black line represents the original distribution, evaluated from a direct simulation of the flow over 2×10^5 turn-over times. In both cases, the algorithm was used with 128 replica, with a cloning period of 0.5 turn-over times. **Left** : time-averaged drag over 400 turn-over times obtained with the algorithm with $k = 0.15$. In this case the large deviations regime is attained and the generated fluctuations are close to $\lambda'(k) \approx 0.1$. **Right** : time-averaged drag over 20 turn-over times obtained with the algorithm with $k = 0.3$. Even if the large deviations regime is **not** attained in this case, the algorithm still generates trajectories related to rare fluctuations. However the typical value of these fluctuations cannot be directly linked to the value of k.

The previous results were obtained in the limit where the drag is averaged over a time much longer than the timescale of typical drag fluctuations, so that the large deviations principle (5) can be established. If this is so, the algorithm gives access to an estimate of the SCGF and there is a direct connection between the value of the bias k and the typical values of the fluctuations related to the generated trajectories. Nevertheless, equation (2) remains valid for shorter trajectories, with this difference that the normalisation factor in (2) cannot be linked to the SCGF in that case. Figure 6 illustrates that the algorithm generates trajectories related to rare fluctuations of the time-averaged drag even if the large deviation regime is not attained.

5 Perspectives

The application of importance sampling described in section 2 to the simple test flow presented in section 3 indicates that such rare event sampling algorithms are relevant for computing rare events in

turbulent flows. We computed the statistics for the extreme fluctuations of the time-averaged drag on the obstacle with only a fraction of the cost required for an estimation with a direct numerical simulation. Furthermore, we simulated the dynamics related to these extreme fluctuations.

Using the algorithm, we will conduct extensive study of the fluid mechanics aspects of the dynamics leading to extreme drag fluctuations based on the generated trajectories. We also look towards complex geometries and applications to industrial flows to simulate rare events of industrial interest. Finally, we will use the algorithm to compute *return times*, indicating the average time one has to wait to witness a given fluctuation. We expect it will be particularly useful for industrial applications.

Acknowledgements The research leading to these results has received funding from the European Research Council under the European Union's seventh Frame- work Programme (FP7/2007-2013 Grant Agreement No. 616811) (F. Bouchet, and T. Lestang). Simulations have been performed on the local HPC facilities at Ecole Normale Supérieure de Lyon (PSMN). These HPC facilities are supported by the Auvergne-Rhône-Alpes region (GRANT CPRT07-13 CIRA) and the national Equip@Meso grant (ANR-10-EQPX-29-01).

Références

[1] Peter G Bolhuis, David Chandler, Christoph Dellago, and Phillip L Geissler. Transition path sampling : Throwing ropes over rough mountain passes, in the dark. *Annual review of physical chemistry*, 53(1) :291–318, 2002.

[2] Olivier Cadot, A Courbois, D Ricot, Tony Ruiz, F Harambat, V Herbert, R Vigneron, and J Délery. Characterisations of force and pressure fluctuations of real vehicles. *International Journal of Engineering Systems Modelling and Simulation*, 8(2) :99–105, 2016.

[3] David Chandler. Interfaces and the driving force of hydrophobic assembly. *Nature*, 437(7059) :640–647, September 2005.

[4] Hudong Chen, Shiyi Chen, and William H. Matthaeus. Recovery of the navier-stokes equations using a lattice-gas boltzmann method. *Phys. Rev. A*, 45 :R5339–R5342, Apr 1992.

[5] Weinan E, Weiqing Ren, and Eric Vanden-Eijnden. Energy landscape and thermally activated switching of submicron-sized ferromagnetic elements. *Journal of Applied Physics*, 93(4) :2275–2282, February 2003.

[6] Zhaoli Guo, Chuguang Zheng, and Baochang Shi. Discrete lattice effects on the forcing term in the lattice boltzmann method. *Phys. Rev. E*, 65 :046308, Apr 2002.

[7] R. V. Kohn, M. G. Reznikoff, and E. Vanden-Eijnden. Magnetic Elements at Finite Temperature and Large Deviation Theory. *Journal of Nonlinear Science*, 15(4) :223–253, June 2005.

[8] Pedro G Lind, Iván Herráez, Matthias Wächter, and Joachim Peinke. Fatigue load estimation through a simple stochastic model. *Energies*, 7(12) :8279–8293, 2014.

[9] Philipp Metzner, Christof Schütte, and Eric Vanden-Eijnden. Illustration of transition path theory on a collection of simple examples. *The Journal of Chemical Physics*, 125(8) :084110, August 2006.

[10] Patrick Milan, Matthias Wächter, and Joachim Peinke. Turbulent character of wind energy. *Phys. Rev. Lett.*, 110 :138701, March 2013.

[11] Fabio Minciarelli, Massimiliano Gioffrè, Mircea Grigoriu, and Emil Simiu. Estimates of extreme wind effects and wind load factors : influence of knowledge uncertainties. *Probabilistic Engineering Mechanics*, 16(4) :331 – 340, 2001.

[12] Takahiro Nemoto, Freddy Bouchet, Robert L. Jack, and Vivien Lecomte. Population-dynamics method with a multicanonical feedback control. *Phys. Rev. E*, 93 :062123, Jun 2016.

[13] Frank Noé, Illia Horenko, Christof Schütte, and Jeremy C Smith. Hierarchical analysis of conformational dynamics in biomolecules : transition networks of metastable states. *The Journal of chemical physics*, 126(15) :04B617, 2007.

[14] Georgios Rigas, Aimee S. Morgans, and Jonathan F. Morrison. *Stability and Coherent Structures in the Wake of Axisymmetric Bluff Bodies*, pages 143–148. Springer International Publishing, Cham, 2015.

[15] Christian M. Rohwer, Florian Angeletti, and Hugo Touchette. Convergence of large-deviation estimators. *Phys. Rev. E*, 92 :052104, Nov 2015.

[16] Sauro Succi. *The lattice Boltzmann equation : for fluid dynamics and beyond*. Oxford university press, 2001.

[17] Hugo Touchette. The large deviation approach to statistical mechanics. *Physics Reports*, 478(1) :1–69, 2009.

[18] Matthias Wächter, Hendrik Heißelmann, Michael Hölling, Allan Morales, Patrick Milan, Tanja Mücke, Joachim Peinke, Nico Reinke, and Philip Rinn. The turbulent nature of the atmospheric boundary layer and its impact on the wind energy conversion process. *Journal of Turbulence*, (13) :N26, 2012.

[19] Pieter Rein ten Wolde and Daan Frenkel. Enhancement of Protein Crystal Nucleation by Critical Density Fluctuations. *Science*, 277(5334) :1975–1978, September 1997.